10th Annual Workshop Prize-Winning Posters

Evidence of spinodal decomposition in semi-crystalline polymers

E.L.Heeley[a], W.Bras[b], I.P. Dolbnya[b], A. Maidens[c], P.D.Olmsted[c]
J.P.A. Fairclough[a] & A.J. Ryan[a].

a Chemistry Department, University of Sheffield, Brook Hill, Sheffield, S3 7HF, UK.
b ESRF, BP220, F-38043, Grenoble Cedex, France.
c IRC, Physics Department, University of Leeds, Leeds, LS2 9JT, UK.

Introduction

Polymer processing relies on the shaping of molten polymer in dies and moulds. During processing, the crystallinity of the material will develop and stabilize the shape of the final product, as well as determining the aesthetic and mechanical properties. Inevitably, the prediction and control of the crystallization of a polymer during its processing will enable new 'application specific' materials to be developed. Clearly, today, the polymer processing industry is concerned with such developments of new and useful materials, due to the high demand for these products in our everyday lives.

The complete processing of a polymer into a product, involves the development of a molecular hierarchical ordered structure (the crystallization process). Here, from the polymer melt, crystallites form and grow into lamellar (crystalline and amorphous regions) which, in turn, are organized into large spherulitic superstructures. The growth of lamellae crystals into the final spherulitic macrostructure is well understood and the theories predicting the crystallization kinetics are usable and well developed [1,2]. However, one area that is less understood in the crystallization process is the 'early' or 'pre-nucleation' stage. Revealing the initial step of polymer crystallization will give a fuller picture of the complete process and provide invaluable information into refining and controlling the final physical properties of the material.

The classical picture of polymer crystallization involves, firstly, the creation of a stable nucleus from the entangled polymer melt and, secondly, the growth of the crystalline region into the lamellar structures and beyond. In the past, the kinetics involved with the formation of a stable nucleus have been difficult to follow experimentally, thus few theories were developed which describe this process well. Recently, however, investigations into the early stages of polymer crystallization X-ray scattering techniques have allowed theories to be developed which describe the process in terms of a 'liquid-liquid' phase separation system[3]. The early stages of the crystallization are thought to follow an ordering of the molecules through a mesophase, which continues to evolve through a process of phase separation into crystalline and amorphous regions. The development of a mesophase in the phase separation process can be described theoretically with the kinetics of spinodal decomposition[4]. Here, a continuous transformation of a partially ordered phase (polymer chains with the correct conformation) develops towards more ordered states leading to nucleation of crystallites and growth. Molecular chains without the correct conformation will become the amorphous phase components. Figure 1, shows how the phase separation leads from the random coil of a polymer melt to a crystalline lamellar structure.

Following the early stages of crystallization kinetics has been successfully reported recently on a range of semi-crystalline polymer samples such as polyethylene terephthalate (PET)[5], isotactic polypropylene (iPP), polyethylene (PE)[6] and polyether ketone ketone (PEKK)[7]. These investigations have also observed spinodal-like
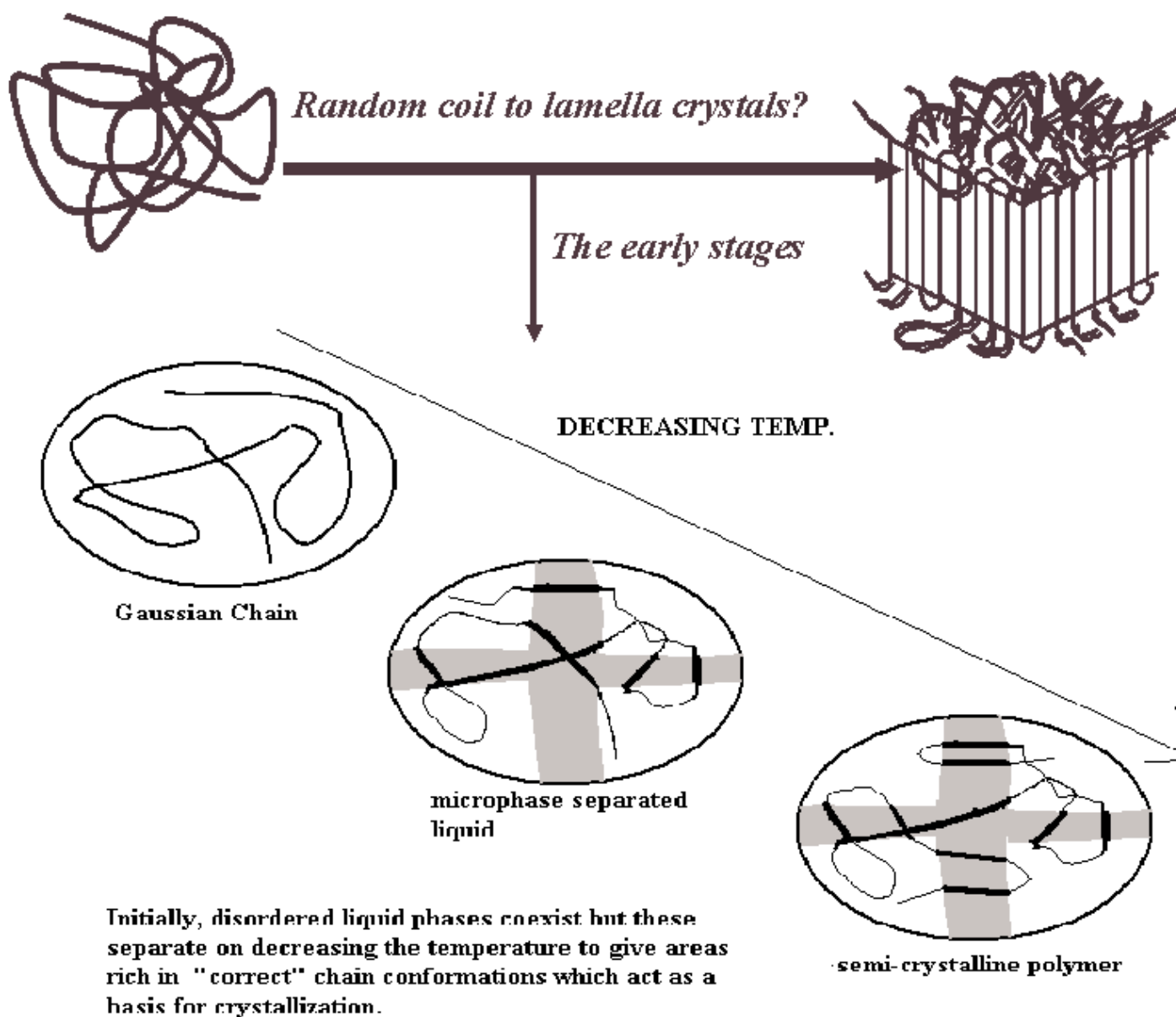
Figure 1: Phase separation during the early stages of polymer crystallization.

kinetics during the early stages of crystallization. Further investigations into the crystallization of commercial iPP samples have been preformed here, using time resolved Small- and Wide- Angle X-ray Scattering experiments. Particular attention has been paid to the early stages of crystallization and relating this to the spinodal decomposition kinetics described.

From the scattering data obtained during crystallization, SAXS develops showing long range ordering (stacking of lamellae) or the macrostructure, along with WAXS giving details on the atomic unit cell or microstructure development. If the kinetics follow classical nucleation and growth theories then the SAXS and WAXS should develop together after an induction period, t_i. However, if the SAXS is seen to emerge before any WAXS is detected during this induction period, then the

development of some long-range ordering must be occurring before any crystalline structure arises. This is identified as the spinodal region during the pre-nucleation stages of crystallization. As the SAXS intensity grows in this period, the kinetics of the crystallization can be fitted to the Cahn-Hilliard (CH) linearized growth model [8,9] for spinodal decomposition. This describes the time evolution of the scattering intensity following an exponential growth from the increased amplification of density fluctuations. The fitting of the CH theory to the SAXS data gives an extrapolated value for the spinodal temperature. Below this temperature the polymer is said to spontaneously separate into two phases.

Previous experimental evidence of spinodal decomposition in iPP and other semi-crystalline polymers has been reported in Ryan *et al.*1999 [10].

Here the spinodal temperatures have been obtained from the CH analysis of SAXS data obtained from the Daresbury SRS. However, recent arguments have questioned this 'phase separation' route to early structure development indicating that scattering observed in the SAXS pattern before WAXS is a feature relating to detector sensitivity [11]. This is, in fact, a valid argument and depends upon the WAXS detector limitations, whether being 'counting rate' or 'intrinsic experimental' limitations. Detector count rates can vary depending on type, but statistical limitations occur when the sum of detected scattered photons is dependant primarily on the scattering process (i.e. lowest detectable crystalline limit).

Recently, improved detector technology has been developed to greatly reduce limitations on 'count rates', allowing improved data collection which can be used in comparison with previous data and so address the issue of WAXS detection capabilities. Details of the early stages of the quiescent crystallization of iPP using time-resolved SAXS/WAXS/DSC experimental techniques, are given below. The data have been collected for comparative examination from both the ESRF Dubble beam line, France and the Daresbury SRS 8.2 beam line, UK using different WAXS detection systems.

Experimental

Samples of commercial iPP (S-30-S:M_w=520Kg/mol., M_w/M_n = 4.4 & Daplen: M_w= 622 Kg/mol, M_w/M_n= 5.5) free from additives, were used to investigate the early stages of quiescent crystallization at several temperatures. Samples were isothermally crystallized having been quenched from above the melting point to the desired temperature, using a Linkam DSC [12]. The SAXS /WAXS data were recorded simultaneously during the crystallization, where similar quadrant SAXS detectors were used [13], however the WAXS detectors differed. The WAXS detector used at the Daresbury SRS (Inel) [13] and the ESRF (MSGC) [14,15] are both photon counting devices and a comparison of their specifications is given in Table 1. The SAXS data from the experiments were analysed using the CH model and the spinodal temperature thus obtained.

Data analysis and results

During the crystallization of the iPP the SAXS/WAXS data were recorded. Figure 2, gives the 1-D SAXS and WAXS data for the quiescent crystallization at 130°C obtained from Dubble at the ESRF. Figure 3 shows the integrated intensity, SAXS from the invariant and WAXS from the relative crystallinity. An Avrami plot is also given which illustrates the slope or the Avrami exponent, in this case the value being ~3 showing a spherulitic grow component [14]. From this figure it is clear that the evolution of SAXS and WAXS are simultaneous. However, Figure 4 gives the integrated intensity of a quiescent crystallization at 142°C. Here, it is clear that the SAXS starts to develop well before any WAXS is observed (a gap of ~10 minutes). During this period, the SAXS peak is seen to grow, indicating the development of long range order. The development of the 1-D SAXS pattern without accompanying WAXS, during the early stages of the crystallization at 142°C, is shown in Figure 5.

The theory of spinodal decomposition is used to describe these events prior to nucleation. The SAXS peak is therefore analysed in terms of the CH model. This predicts that the variation in the scattering intensity with time following a quench, is given by the following equation:

$$I(q,t) = I_0 e^{2R(q)t} \qquad (1)$$

Being:

$$R(q) = D_{eff}\, q^2 \left[\frac{1-q^2}{2q_m^2}\right] \qquad (2)$$

Where, I_o is the initial scattering intensity, $R(q)$ is the growth rate at given q, D_{eff} is the effective diffusion coefficient and q_m the wave vector having the highest rate of growth.

The growth rate $R(q)$ is determined by plotting lnI vs t, for discrete wave vectors and obtaining the slope. From this the CH plots $(R(q)/q^2$ vs $q^2)$ are performed and extrapolation of $q=0$ of the linear portion (between the limits $q_m<q<\sqrt{2}q_m$) of the plot gives D_{eff}. Figure 6 gives an example of the CH plot of the crystallization at 142°C during the spinodal region. The inset shows the scattering intensity at discrete values of q with time, where the linear slope gives
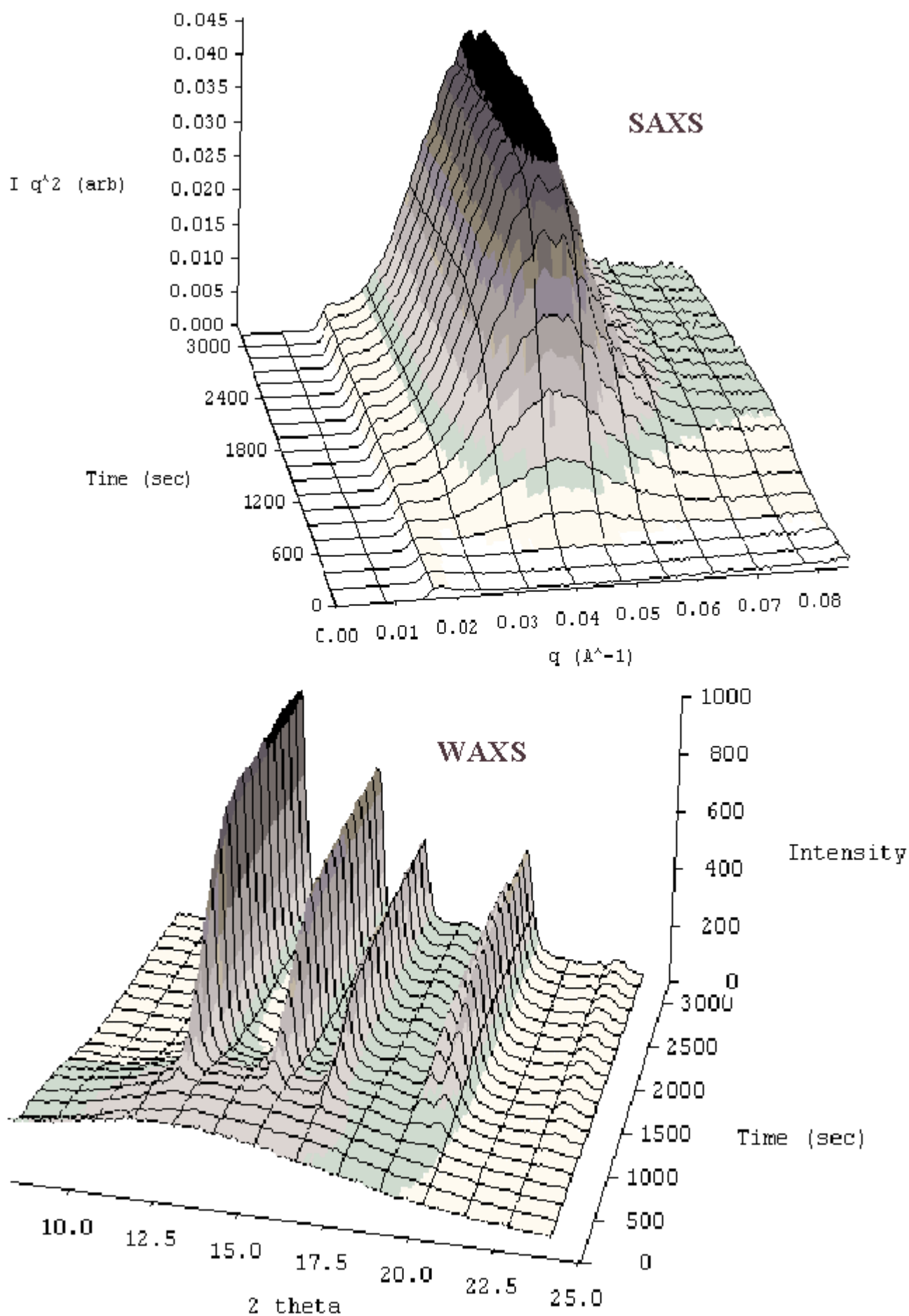
Figure 2: SAXS/WAXS development during quiescent crystallization of iPP at 130ºC.
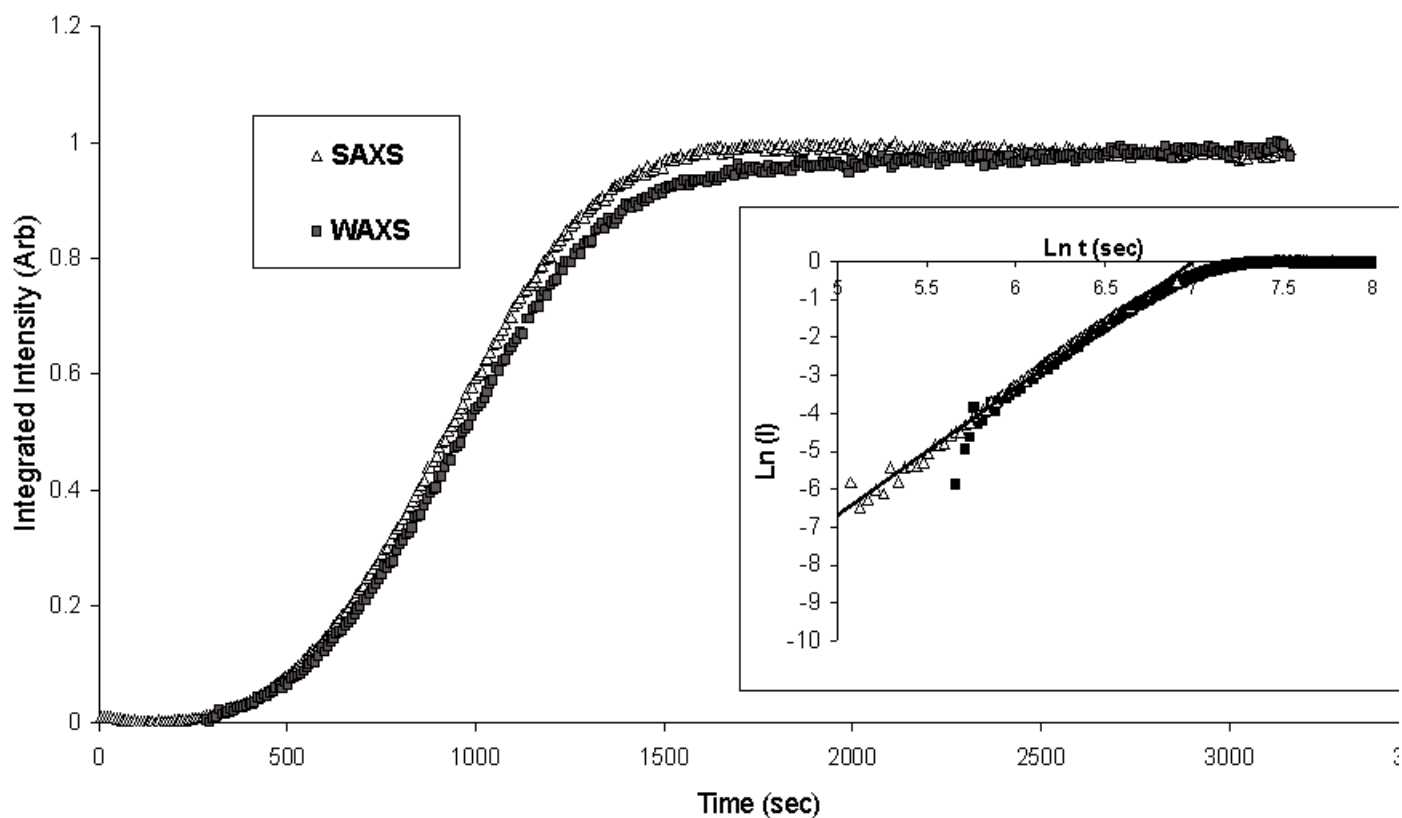
Figure 3: Integrated intensity data for quiescent crystallization of iPP at 130oC. Inset illustrates Avrami plot where the fit has a slope ~3.
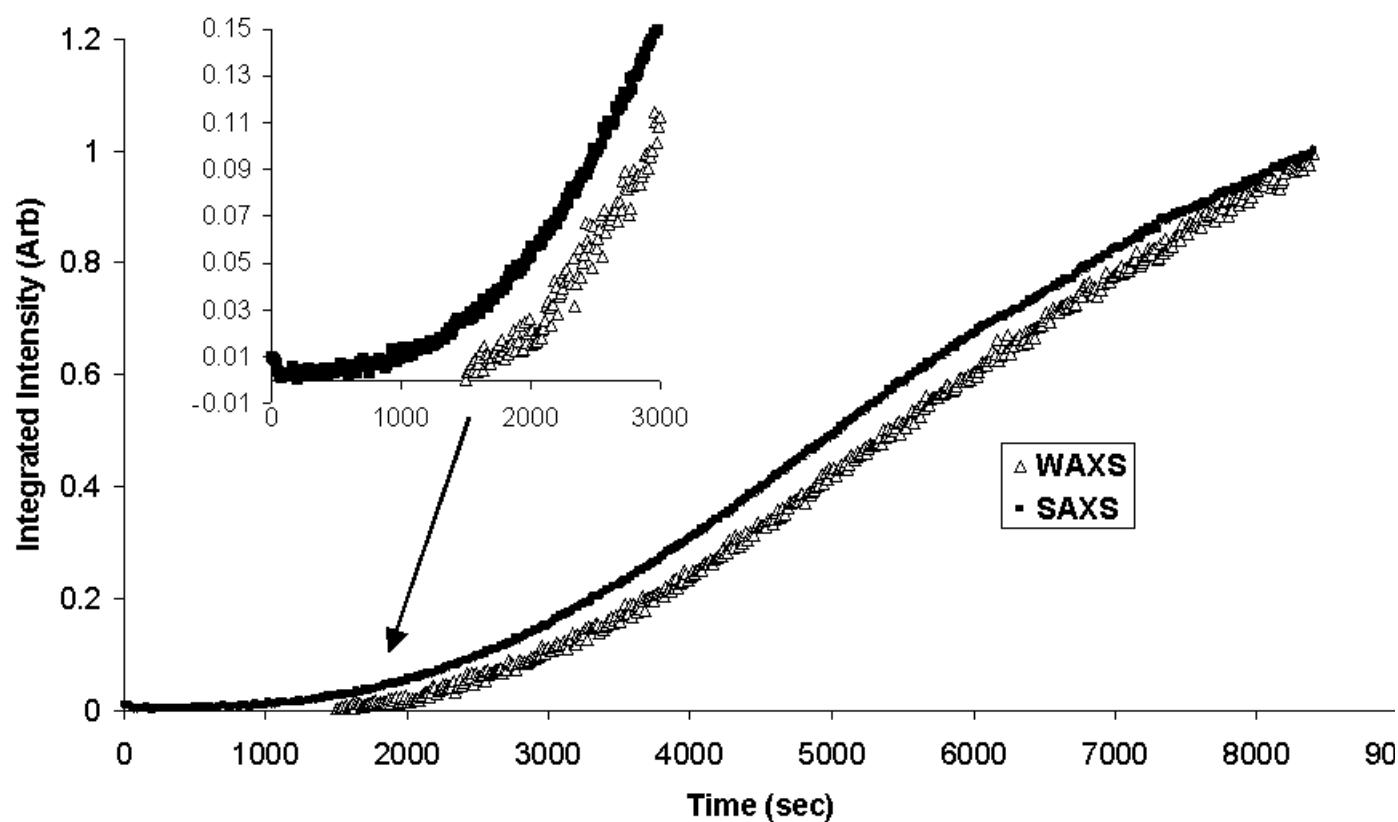

Figure 4: Integrated intensity of quiescent crystallization for iPP at 142ºC. Inset shows development of SAXS before WAXS. Here, SAXS intensity is shown at t = 0 but, no WAXS peaks develop to integrate before 1500s.
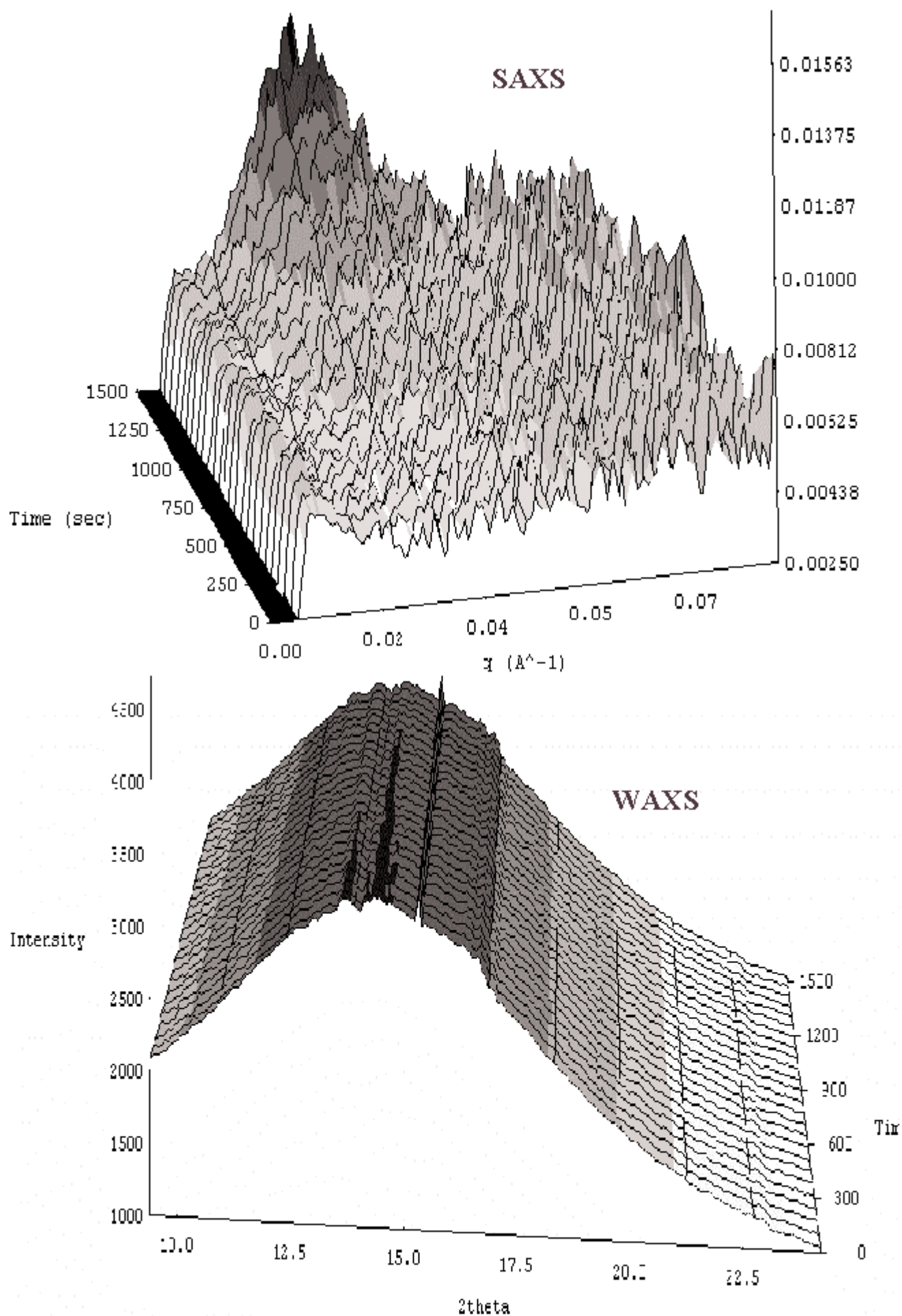
Figure 5: Development of SAXS peak before WAXS during the spinodal region.
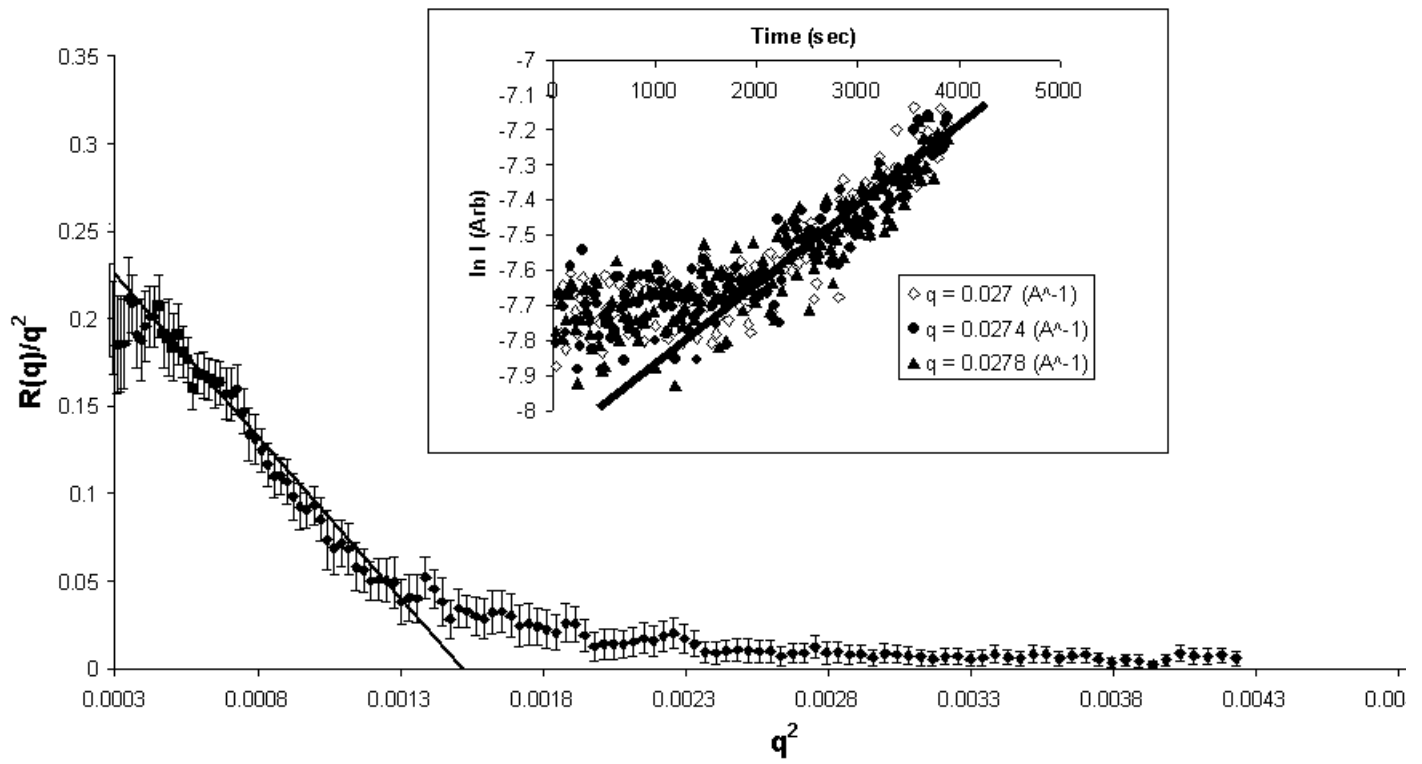
Figure 6: Cahn-Hilliard plot of quiescent crystallization of iPP at 142ºC where the linear fit is used to estimate D_{eff} at $q=0$. The inset shows LnI v t plots for discrete values of q, here the linear fits are used to calculate $R(q)$.
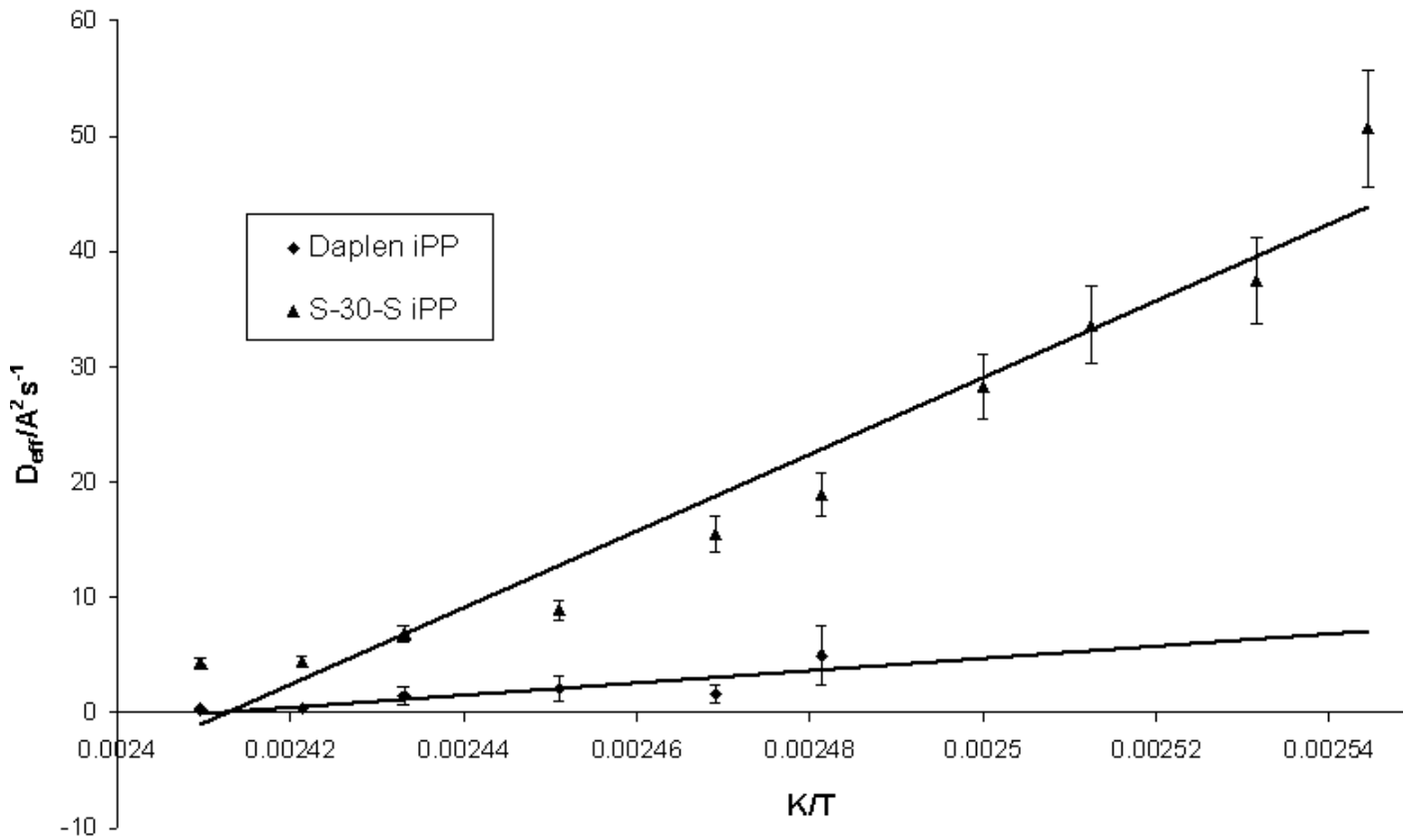

Figure 7: Graph of D_{eff} v $1/T$, allowing the calculation of the spinodal temperature from extrapolation to $D_{eff}=0$

the growth rate $R(q)$. The D_{eff} values at several quench temperatures were calculated in this way for the polypropylene sample in order to estimate the spinodal temperature Ts. Figure 7, shows a plot of the D_{eff} values with quench temperatures for the two similar iPP samples, S-30-S where the data were recorded at the Daresbury SRS (from Ryan *et al*. 1999) and Daplen having data recorded from the ESRF. Table 2 gives the spinodal temperature which is calculated from the extrapolation of $D_{eff} = 0$, along with the thermodynamic melting point T_{m0} [15] and measured DSC melting point T_m. From the table the T_s values of both iPP samples are estimated to be 415 K, which is 44 K below the thermodynamic melting point of a polypropylene crystal and ~23 K below the measured melting point. The final long spacing of the polypropylene from the SAXS is ~150Å.

Discussion

Crystallizations with long induction times, i.e. shallow quench temperatures, show evidence of the onset of long scale ordering prior to crystal growth from simultaneous SAXS/WAXS experiments. It has been possible to analyse the data in terms of spinodal decomposition theory, where the events are described as a phase separation process and the amplitude of the density fluctuation increases with time , shown by the early emergence of a SAXS peak before WAXS. The SAXS data can be conveniently fitted to the Cahn-Hilliard model which gives rise to the spinodal temperature, below which the polymer spontaneously separated into two phases. From the data taken using similar iPP samples but using different WAXS detectors, some differences have been observed in the results with respect to the quench temperature. Generally, the gap between SAXS and WAXS is seen to agree with data obtained from both WAXS detectors at shallow quench depths. However, the gap is not observed at deep quench depths in the data obtained from the MSGC detector at the ESRF. This indicates that the improved signal to noise ratio in the MSGC detector allows the detection of crystallinity from the sample at lower levels than does the Inel detector.

In conclusion, agreement with T_s values has been observed with both systems, but obviously improvements in detector technology have led us to address the argument of detector sensitivity. It is possible now to see how the improvements made with the MSGC detector have enabled the issue of spinodal decomposition as a precursor to nucleation to still be an obvious route to primary crystallization. However, experimentally, the phase separation is very much a temperature dependant process and even though we have seen that the technical detector limitations are reduced from the comparison of data here, there are still statistical limitations in the data analysis that cannot be totally disregarded.

References

[1]   Young, R.J. & Lovell, P.A., *Introduction to Polymers*, Chapman & Hall, London, 2nd ed, 1991.

[2]   Gedde, U.W. *Polymer Physics*, Chapman & Hall, London, !st edition, 1995.

[3]   Olmsted, P.D., Poon, W.C.K., McLeish, T.C.B.,Terrill, N.J.& Ryan, A.J., *Phys Rev. Letters* , 1998, **81** , 373-376.

[4]   Bates, F. S. & Wiltzius, P. , *J. Chem. Phys.* , 1989, **91** , 3258-3274.

[5]   Imai, M., Kaji, K. & Kanaya, T., *Macromols*., 1994, **27**, 7103-7108.

[6]   Terrill, N. J., Fairclough. P. A., Towns-Andrews, E., Komanschek, B. U., Young, R. J., Ryan, A. J., *Polymer*, 1998, **39**, 2381.

[7]   Ezquerra, T.A.,López-Cabarcos, E., Hsiao, B. S. & Baltà-Calleja, F. H., *Phys. Rev. E* , 1996 , **54**, 989--992 .

[8]   Cahn, J. W., Hilliard, J.E., *J. Chem. Phys.*, 1958, **28**, 25.

[9]   Gunton, J. D., San Miguel, M., Sahni, P. S. *In Phase Transitions and Critical Phenomena*; Domb, C., Green, M. S., Eds.; Academic: New York, 1983; **8**.

[10] Ryan, A. J., Fairclough. P. A., Terrill, N. J., Olmsted, P.D., Poon, W.C.K., *Faraday Discuss.*, 1999, **112**, 13.

[11] Wang, Z. G., Hsiao, B.S., Sirota, E.B., Agarwal, P & Srinivas, S., *Macromols*., 2000, **33**, 978-989.

[12] Bras, W.; Derbyshire, G. E.; Mant, G. R.;

Clarke, S. M.; Cooke, J.; Komanschek, B. U.; Ryan, A. J. *J. Appl. Cryst.* 1994, **28**, 26.

[13] Bras, W.; Derbyshire, G. E.; Ryan, A. J.; Mant, G. R.; Felton, A.; Lewis, R. A.; Hall, C. J.; Greaves, G. N. *Nucl. Instrum. Methods Phys. Res.* 1993, **A326**, 587.

[14] Bras, W.; *J. Macromol. Sci.-Phys.* 1998, **B37(4)**, 557.

[15] Zhukov, V.; Udo, F.; Marchena, O.; Hartjes, F. G.; van den Berg. F. D.; Bras, W.; Vlieg, E.; *Nucl. Instrum. Methods Phys. Res.* 1997, **A392**, 83.

[16] Avrami, M., J. Chem. Phys., 1939, 7, 1103; ibid, Avrami, M., *J. Chem. Phys.*, 1940, **8**, 212.

[17] Mark, J.E. *Physical properties of polymers*, American Institute of Physics, NY, 1996.